Journal of Environmental Management 370 (2024) 122605

Contents lists available at ScienceDirect

Journal of Environmental Management

journal homepage: www.elsevier.com/locate/jenvman

Research article

New insights into evodiamine attenuates IPEC-J2 cells pyroptosis induced by T-2 toxin - Activating Keap1-Nrf2/NF-κB signaling pathway through binding with Keap1

Tingting Yu [a], Xinrui Deng [a], Xuejiao Yang [a], Yilin Yin [a], Yong Liu [b,**], Shiwen Xu [a,c,*]

[a] College of Veterinary Medicine, Northeast Agricultural University, Harbin, 150030, PR China
[b] Mudanjiang Medical University, Mudanjiang, 157011, PR China
[c] Key Laboratory of the Provincial Education Department of Heilongjiang for Common Animal Disease Prevention and Treatment, College of Veterinary Medicine, Northeast Agricultural University, Harbin, 150030, PR China

ARTICLE INFO

Keywords:
T-2 toxin
Evodiamine
Keap1-Nrf2/NF-κB signaling pathway
Porcine intestinal epithelial J2 cell
Pyroptosis

ABSTRACT

T-2 toxin (T-2) is a highly toxic mycotoxin with a molecular weight of 466.52 g/mol. Evodiamine (EV), an alkaloid component of Evodia, has anti-inflammation and antioxidant properties. As a receptor of oxidative stress, Keap1 with a molecular weight of 70 kDa, is a molecular switch that controls the Nrf2 signaling pathway. In this paper, the effect of EV on Keap1-Nrf2/NF-κB pathway was investigated. Based on our research outcomes, it was observed that T-2 exposure substantially increased IPEC-J2 cells intracellular ROS levels and MDA accumulation, decreased SOD and CAT activities, disrupted intestinal tight junction (ZO-1, occludin, and claudin-1), and up-regulated pyroptosis-related protein (ASC, NLRP3, caspase-1, GSDMD, IL-1β, and IL-18). Additionally, EV could bind well with Keap1, the separating it from Nrf2, promoting Nrf2 into the nucleus, enhanced antioxidant enzyme activities, reduced the production of ROS, down-regulated NF-κB expression, alleviated T-2-induced pyroptosis, and restored tight junction protein expression. However, after treatment with the Nrf2 inhibitor ML385, ML385 reversed the protective effect of EV on IPEC-J2 cells. Collectively, EV can activate the Keap1-Nrf2/NF-κB signaling pathway via binding to Keap1, exert anti-inflammatory and antioxidant effects, inhibit the pyroptosis of IPEC-J2 cells triggered by T-2, and retore intestinal barrier function.

1. Introduction

T-2 toxin (T-2) is categorized as a type A trichothecenes toxin produced by *Fusarium* (Mateo, Mateo et al. 2002), which has the properties of non-volatilization, high-temperature resistance, light resistance, inactivation under strong acid and alkali conditions (Li et al., 2011; Zhang, Song et al. 2024a). At present, of all the grains tested, maize, wheat, oat, and rye are susceptible to T-2 contamination (Mahato, Pandhi et al. 2022). In a study of 420 feedstuff samples from China, it was found that the incidence of T-2 exhibited a remarkably high value of 79.5% and its level ranged from 10 to 735 μg/kg (Wang, Liu et al. 2013). T-2 is approximately tenfold higher virulent than deoxynivalenol (Ueno, 1984). Studies have suggested that the liver is the primary target of T-2, as well as thymus and spleen are its potential targets (Čonková, Laciakova et al. 2003; Song, Wang et al. 2023). Additionally, T-2 can inhibit mitochondrial function, disrupt the synthesis of RNA, DNA, and protein synthesis, and exhibit cytotoxic and immunosuppressive effects (Shi, Li et al. 2018). When ingested by animals, T-2 can lead to erythrocyte damage, liver and gastrointestinal tract damage, decreased blood glucose, lead to loss of weight, and growth retardation (Nathanail, Varga et al. 2015; Adhikari, Negi et al. 2017). T-2 could inhibit reproductive hormone synthesis and eventually lead to reproductive dysfunction (Yang, Liu et al. 2020). Swine have been identified as the species with the highest sensitivity to T-2, second by poultry, while ruminants are the least sensitive due to the protective effect of microflora (Streit et al., 2012). Dietary supplementation of antioxidants can prevent T-2-induced acute toxicosis (Rizzo, Atroshi et al. 1994). It has been demonstrated that NaClO inhibits biological activity, so it is called a decontaminant for T-2 (Adhikari, Negi et al. 2017).

Nuclear factor erythroid 2-related factor 2 (Nrf2), an autoregulator

* Corresponding author. College of Veterinary Medicine, Northeast Agricultural University, Number 600, Changjiang Street, Harbin, 150000, PR China.
** Corresponding author. Mudanjiang Medical University, No.3, Tongxiang Street, Aimin District, Mudanjiang, 157011, PR China.
E-mail addresses: liuyong@mdjmu.edu.cn (Y. Liu), shiwenxu@neau.edu.cn (S. Xu).

https://doi.org/10.1016/j.jenvman.2024.122605
Received 16 July 2024; Received in revised form 30 August 2024; Accepted 17 September 2024
Available online 20 September 2024

of the antioxidant stress, prevents oxidant stress (OS) and inflammation. Under normal physiological conditions, Nrf2 binds to Kelch-like ECH-associated protein1 (Keap1, an important regulator of OS) in the cytoplasm and continuously degrades by ubiquitination, so that it cannot enter the nucleus to exert transcriptional activity. When the conformation of Keap1 is changed by OS and electrophile substances, Nrf2 is activated after dissociation from Keap1. The activated Nrf2 enters the nucleus, forming a complex with antioxidant response element (ARE). Then, the downstream antioxidant protein and ubiquitin-proteasome system genes are activated to maintain the oxidation-reduction balance of cells. However, over-activated Nrf2 can increase the proliferative activity of cancer cells, promote tumor development (De Nicola, Karreth et al. 2011; Onodera, Motohashi et al. 2014), and improve the tolerance of cancer cells to chemotherapeutics (Kansanen, Kuosmanen et al. 2013). Nuclear factor-kappa B (NF-κB) holds a significant importance in regulating immune response and inflammation(Gao, Yang et al. 2022a,b; Li et al., 2023). Normally, the cytoplasm NF-κB, a dimer of protein components (p50/p65), binds to the inhibitor of NF-κB (IκB) to establish a trimer complex and is inactivated. When stimulated by tumor necrosis factor-alpha (TNF-α), lipopolysaccharide (LSP), interleukin-1 beta (IL-1β), etc., the classical pathway of NF-κB will be activated. These signals activate the IκB-kinases (IKK), resulting in phosphorylation of the NF-κB inhibitor alpha (IκBα), which is dissociated from the heterotrimer and degraded by the proteasome after ubiquitination modification and then the activated NF-κB is promptly moved into the nucleus, where it initiates or augments its function associated genes transcription. Overactivation of NF-κB is able to induce inflammation and tumor development (Dolcet, Llobet et al. 2005; Barnabei, Laplantine et al. 2021). There is a complex interaction between Nrf2 and NF-κB, and loss of Nrf2 enhances NF-κB activity, while NF-κB is able to regulate the transcription and activity of Nrf2 (Wardyn, Ponsford et al. 2015). The balance of antioxidant and inflammatory responses can be altered by complex interactions between Nrf2 and NF-κB signaling pathways (Sivandzade, Prasad et al. 2019; Jing, Wang et al. 2022). Pyroptosis is a cellular inflammatory necrosis mediated by proteins of the gasdermin family and characterized by inflammasome activation, cell membrane perforation, and cell rupture (Yu et al., 2021). NF-κB activated can activate the classic pyrin domain containing 3 (NLRP3) inflammasome, and reactive oxygen species (ROS) is essential to regulate NF-κB activity (Dong, Yang et al. 2024; Li et al., 2024; Lu et al., 2024; Zhang, Zhang et al. 2024b). Therefore, antioxidant products can prevent inflammation and pyroptosis by increasing the activity of Nrf2, thereby reducing ROS production and preventing gasdermin D (GSDMD) and NF-κB activation (Ahmed, Luo et al. 2017; Hurtado-Navarro, Angosto-Bazarra et al. 2022; Rousta, Mirahmadi et al. 2022).

Evodiamine (EV), an indole alkaloid isolated from *Evodia rutaecarpa* (Yu et al., 2013), has pharmacological activities including anti-tumor, anti-microbial, and anti-inflammatory (Ogasawara, Matsunaga et al. 2002; Jiang and Hu, 2009). Studies have shown that EV could alleviate mouse mastitis through down-regulating AKT/NF-κB p65 and MAPK signaling and inhibiting pro-inflammatory mediators production (Yang, Ran et al. 2022). Studies by Lei et al. have confirmed that EV can reduce the apoptosis in hepatocytes of grass carp produced by di (2-ethylhexyl) phthalate (DEHP) (Lei, Zhang et al. 2023). However, it is unclear whether EV has the mitigating effect on enterotoxicity caused by T-2 toxin. Thus, the IPEC-J2 cells exposure to T-2 were used as the in vitro culture model in the present research, ROS fluorescence probe, OS kits, cellular immunofluorescence staining, quantitative real-time PCR (qRT-PCR) analysis, and Western blotting detected the OS levels, sate of intestinal tight junction, Keap1-Nrf2-/NF-κB signaling and pyroptosis-related molecule expression. Meanwhile, using Matescape and STRING evaluated the correlation between Keap1-Nrf2-/NF-κB signaling pathway, pyroptosis and intestinal tight junction. The molecular docking method investigated the interaction between EV and Keap1. This study aims to provide new insights into the underlying mechanism of cytotoxic effects of T-2 on IPEC-J2 cells, elucidate the mechanism of EV in alleviating cell damage caused by T-2, and provide a new therapeutic strategy for the detoxification of T-2.

2. Materials and methods

2.1. Cell culture and viability analysis

The IPEC-J2 cells, presented by the microbiological Professor Lijie Tang research group of Northeast Agricultural University, were grown in DMEM/F12 medium (Gibco, USA) containing 10% fetal bovine serum (FBS, BI, China) and in a 5% CO_2 humidified environment at 37 °C.

The cell viability was identified by using Cell Counting Kit-8 (CCK-8) (Meilunbio, China) assay. The cells were grown in a 96-well plate (8×10^3 cells/well). After cell adhesion, the medium containing different T-2 (Purity ≥97.5%, Macklin, China) concentrations was changed for 24 h. Next, medium containing 10% CCK-8 regent was added to each well and cultured at 37 °C for 1 h. At last, an Infinite F50 microplate reader (TECAN, Switzerland) measured each well' s absorbance at 450 nm. The optimal concentration of T-2 was chosen for the subsequent experiments. Then, the optimal T-2 concentration and different EV (HPLC ≥98%,Meilunbio, China) concentrations co-treatment cells for 24 h. The configuration method of T-2 and EV with different concentrations are as follows. Dissolve T-2 and EV in DMSO (Biosharp, China) to achieve an initial concentration of 100 mg/mL and 100 mM, respectively, and then diluted to the desired concentration with medium. For experiments involving the Nrf2 inhibitor ML385, the drug, inhibitor and cells are co-cultured for 24 h.

2.2. Lactate dehydrogenase (LDH) activity measurement

The IPEC-J2 cells (1×10^6 cells/well) cultured in a 6-well plate with different treatments. LDH activity was measured using the LDH kits (Jiancheng, China).

2.3. Intracellular oxidative stress (OS) levels assay

Intracellular ROS was measured using DCFH-DA (Jiancheng, China). IPEC-J2 cells were inoculated in a 6-well plate (1×10^6 cells/well). After corresponding treatment, cells were washed with PBS and treated using DCFH-DA (diluted with PBS at 1:1000) in darkness at 37 °C. The fluorescence signals were collected by fluorescence microscopy and analyzed using Image J.

The OS indexes superoxide dismutase (SOD), catalase (CAT) and malondialdehyde (MDA) were measured using the corresponding kit according to the manufacturer' s instructions (Jiancheng, China).

2.4. Immunofluorescence staining

IPEC-J2 cells were seeded in a 6-well plate (1×10^6 cells/well) with corresponding treatment for 24 h. Then, cells were washed thrice and fixed overnight at 4 °C with 4% paraformaldehyde. After washed with TBSTx, the cells were blocked with 5% BSA at ambient temperature. After 1.5 h, the cells were washed three times and incubated with diluted anti-GSDMD rabbit antibody (1:200, Abcam, China) overnight at 4 °C and 45 rmp. The cells were treated with Dylight 595-Goat Anti-Rabbit IgG (1:1000, Biodragon, China) for 2 h at 4 °C and 45 rmp in the dark. After rewashing, the cells were treated at 37 °C and 40 rmp with diluted anti-NLRP3 rabbit antibody (1:200, Wanlei, China) in the dark. After 2 h, the cells were rewashed and treated with Dylight 488-Goat Anti-Rabbit IgG (1:1000, Biodragon, China) for 1 h and 45 rmp. Finally, the nucleus was dyed with DAPI (Beyotime, China). The fluorescence signals were collected using fluorescence microscopy and quantized using Image J.

2.5. Quantitative real-time PCR (qRT-PCR) analysis

The mRNA levels of the target gene were measured with qRT-PCR, as the experimental described (Lei, Zhang et al. 2023). The LightCycler® 480 system (Roche, Switzerland) was used to perform the qRT-PCR. With β-actin serving as the reference gene, the expression of target gene was measured by the $2^{-\Delta\Delta CT}$ calculation method. All primers were synthesized by Sangon Biotech (Shanghai, China), as exhibited in Table 1.

2.6. Western blotting analysis

Protein samples were abstracted from IPEC-J2 cells by Western blot/IP lysis buffer (Beyotime, China) and protease inhibitor PMSF (phenyl methane sulfonyl fluoride, Biosharp, China). In addition, following the instructions, the nuclear and cytoplasmic protein extraction kit (Beyotime, China) isolated the proteins of the nucleus and cytoplasm from IPEC-J2.

The expression of the target gene in IPEC-J2 cells was determined with Western blotting, following the experimental procedures described (Yao, Chen et al. 2023). The protein bond was rewashed with TBST and visualized using the ECL chemiluminescent substrate (Biosharp, China) and Azure Biosystems C300 (Azure Biosystems, USA). With β-actin as the total protein and cytoplasmic protein internal reference, and with proliferating cell nuclear antigen (PCNA) as the nuclear protein internal reference, Image J software analyzed each protein expression. The primary anti-rabbit antibodies and their dilution ratios are shown in Table 2.

2.7. Protein-protein interaction (PPI) analysis and enrichment analysis

To visualize the functional PPI networks of differentially expressed protein, swine species were selected, and the PPI networks were performed using the Search Tool for the Retrieval of Interacting Genes (STRING) database. Meanwhile, enrichment analysis was carried out using Metascape Network Tools (http://metascape.org).

2.8. Molecular docking

Molecular docking predicted the possible interaction mode between EV and Keap1 by AutoDock Vina 1.1.2. The UniProt entry of Keap1 is Q684M4 (https://www.uniprot.org/uniprotkb/Q684M4/entry), and Keap1 protein was preprocessed by AutoDock Tools 1.5.6.

The three-dimensional conformation of EV was acquired from the PubChem database (https://pubchem.ncbi.nlm.nih.gov/compound/442088) based on its CAS number. Then, the energy of the small molecule was minimized in Chem 3D 19.0 with a force field of MM2 and RMS Gradient of 0.009. Finally, the optimized small molecule ligand was treated with OpenBabel 2.4.1.

The docking constructs were set to 10. The binding ability of small molecular ligand EV and receptor protein Keap1 was analyzed by molecular docking results. It is generally acknowledged that the higher the binding energy absolute value, the better the binding effect between the small molecular ligand and the protein receptor.

Table 2
Primary anti-rabbit antibodies catalog.

Antibodies	Cat.No	Manufacturer	Diluted multiples
Nrf2	WL02135	Wanlei, Shenyang, China	1:750
Keap1	WL03285	Wanlei, Shenyang, China	1:1500
iκκα	WL00053	Wanlei, Shenyang, China	1:500
NF-κB p65	WL01980	Wanlei, Shenyang, China	1:500
p-NF-κB p65	WL02169	Wanlei, Shenyang, China	1:750
ASC	WL02462	Wanlei, Shenyang, China	1:500
NLRP3	WL02635	Wanlei, Shenyang, China	1:1500
Caspase-1	WL02996	Wanlei, Shenyang, China	1:500
GSDMD	Ab219800	Abcam, shanghai, China	1:1500
IL-1β	WL00891	Wanlei, Shenyang, China	1:500
IL-18	WL01127	Wanlei, Shenyang, China	1:1500
ZO-1	WL03419	Wanlei, Shenyang, China	1:1000
Occludin	WL01996	Wanlei, Shenyang, China	1:1000
Claudin-1	WL03073	Wanlei, Shenyang, China	1:1500
β-actin	bs-0061R	Bioss, Beijing, China	1:10,000
PCNA	WL03213	Wanlei, Shenyang, China	1:1000

2.9. Statistics analysis

Each experiment was conducted at least three times with similar results, and all experimental data were analyzed using GraphPad Prime 9 for one-way analysis of variance (ANOVA). Data are presented as mean ± standard deviation (mean ± SD). A p-value <0.05 was considered statistically significant. The software showed that data had a normal distribution.

3. Results

3.1. EV treatment inhibited T-2-induced cytotoxicity in IPEC-J2 cells

Firstly, the impact of T-2 (1–8 ng/mL) and EV (0.5–8 μM) on the viability of IPEC-J2 cells was assessed using CCK8 and LDH activity assay. As exhibited in Fig. 1A, IPEC-J2 cells viability decreased linearly with increasing T-2 concentration. The average IC_{50} of T-2 exposure for 24 h was 6.314 ng/mL, and the cell viability was 64.4% at a 4 ng/mL T-2. When EV concentration reached 8 μM, there was no apparent toxicity of IPEC-J2 cells, and the cell survival rate dropped to 92.55% (Fig. 1B). Thus, in the subsequent experiment, 4 ng/mL T-2 and 0.5, 1, 2, 4 μM of EV were chosen. To evaluate the impact of EV on the cytotoxicity triggered by T-2, we measured the survival rate of IPEC-J2 cells treated with varying concentrations of EV in the presence of 4 ng/mL T-2. 0.5, 1, 2 μM EV markedly suppressed T-2-induced decrease in cell viability, and the effect of 0.5 μM EV was the most significant ($p < 0.0001$, Fig. 1C). Thus, 4 ng/mL T-2 and 0.5 μM EV were chosen in the LDH releasing

Table 1
The mRNA sequence used in qRT-PCR.

Gene	Accession umber	Primer(5' → 3')	
		Forward	Reverse
Nrf2	XM_013984303.2	AACCAAACCGACAGAAATTGACAAC	TGGAGAGGATGCTGCTGAAGG
NF-κB	NM_001114281.1	CCAGACCAACAACAACCCCTTCC	AAGCAGAGCCGCACAGCATTC
Caspase-1	NM_214162.1	GCCGTGGTGAGAAGCAAGGG	CCAATAAGGGATGTCGCCAAGAAAC
NLRP3	XM_021078922.1	CCAGGACATCCAAGACCACCAC	CGCAGCCAGTGAGCAGAGAC
ASC	XM_003124468.5	ATGCCATCGACCTCACTGACAAG	GCTCCGCCACCTCCTTCATG
IL-1β	NM_214055.1	TGTCATCGTGGCAGTGGAGAAG	TTTGTGGTCTTTGTCCTGGAGTTTG
IL-18	XM_005667326.2	CCGTGTTTGAGGATATGCCTGATTC	GATGGTTACTGCCAGACCTCTAGTG
ZO-1	XM_021098848.1	CCAGGGAGAGAAGTGCCAGTAGG	TTTGGTGGGTTTGGTGGGTTGAC
Occludin-1	XM_005672522.3	CAGTGGTAACTTGGAGGCGTCTTC	CGTCGTGTAGTCTGTCTCGTAATGG
Claudin-1	NM_001244539.1	ACTCCTACGCTGGTGACAACATTG	CGACACGCAGGACATCCACAG
β-actin	XM_021086047.1	TCTGGCACCACACCTTCTACAAC	GTCATCTTCTCACGGTTGGCTTTG

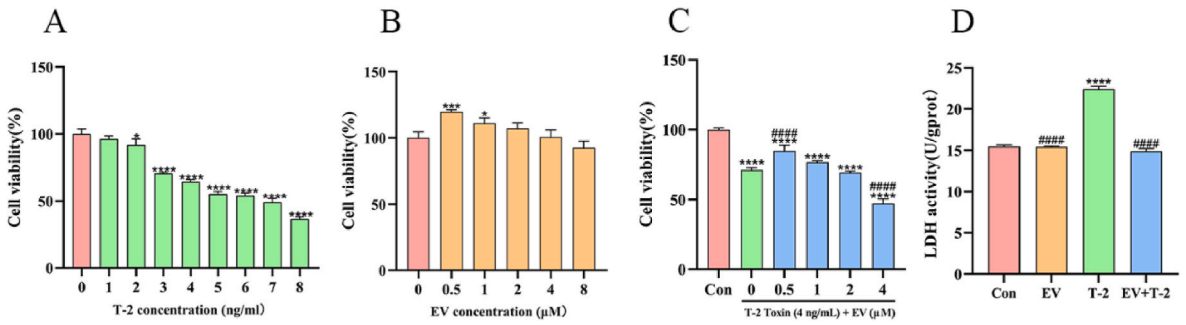

Fig. 1. Effects of T-2 and EV on IPEC-J2 cells. (A–C) The cell viability under different treatments. (D) The LDH activity. Data are presented as mean ± SD (n = 3). *p < 0.05, **p < 0.01, ***p < 0.001 and ****p < 0.0001 vs. control; #p < 0.05, ##P < 0.01, ###p < 0.001 and ####p < 0.0001 vs. T-2.

assay. It was found that 0.5 μM EV markedly suppressed 4 ng/mL T-2-increased in LDH activity ($p < 0.0001$, Fig. 1D). These findings indicated that EV could mitigate T-2-induced cytotoxic effects in IPEC-J2 cells.

3.2. EV treatment relieved T-2-induced oxidative stress in IPEC-J2 cells

To investigate the effect of EV on OS caused by T-2, we measured SOD and CAT activities, and the concentration of intracellular ROS and MDA. As depicted in Fig. 2A, intracellular ROS levels were significantly elevated after T-2 exposure ($p < 0.0001$). Additionally, T-2 exposure markedly increased MDA contents and decreased SOD and CAT activities in IPEC-J2 cells. However, EV treatment could inhibit the increase of T-2-induced OS indicators ($p < 0.0001$, Fig. 2B–D). 0.5 μM EV significantly reduced intracellular ROS and MDA accumulation caused by T-2 and markedly increased antioxidant enzymes (SOD and CAT) activity ($p < 0.0001$). Thus, these findings indicated that EV could alleviate the oxidative stress triggered by T-2 exposure in IPEC-J2 cells.

3.3. EV treatment inhibited T-2-induced pyroptosis in IPEC-J2 cells

To assess the impact of EV on pyroptosis caused by T-2, we conducted an analysis of pyroptosis-associated gene mRNA and protein expression. As demonstrated in Fig. 3A–B, T-2 exposure markedly enhanced ASC, NLRP3, caspase-1, IL-1β, and IL-18 mRNA levels ($p < 0.05$), and up-regulated ASC, NLRP3, caspase-1, GSDMD, IL-1β, and IL-18 proteins expression ($p < 0.0001$). However, after 0.5 μM EV treatment, the above changes were notably reversed. Meanwhile, T-2 alone enhanced the fluorescence intensity of GSDMD and NLRP3 in IPEC-J2 cells ($p < 0.0001$, Fig. 3C). Nevertheless, EV treatment markedly lowered the increases, consistent with previous results. Thus, these findings demonstrated that EV might be beneficial in protecting IPEC-J2 cells from T-2 exposure-induced pyrotosis.

3.4. EV treatment alleviated T-2-induced tight junction disorder in IPEC-J2 cells

To investigate the effect of EV on intestinal tight junction dysfunction induced by T-2, we assessed tight junction-related gene and protein expression. As exhibited in Fig. 4A and B, compared with the control group, the T-2 exposure group dramatically decreased of zonula occludens-1 (ZO-1), occludin, and claudin-1 mRNA and protein expression ($p < 0.05$). Nevertheless, EV treatment reversed these changes induced by T-2 ($p < 0.0001$). Thus, the implication of these results was that EV treatment could alleviate the tight junction dysfunction of IPEC-J2 cells caused by T-2.

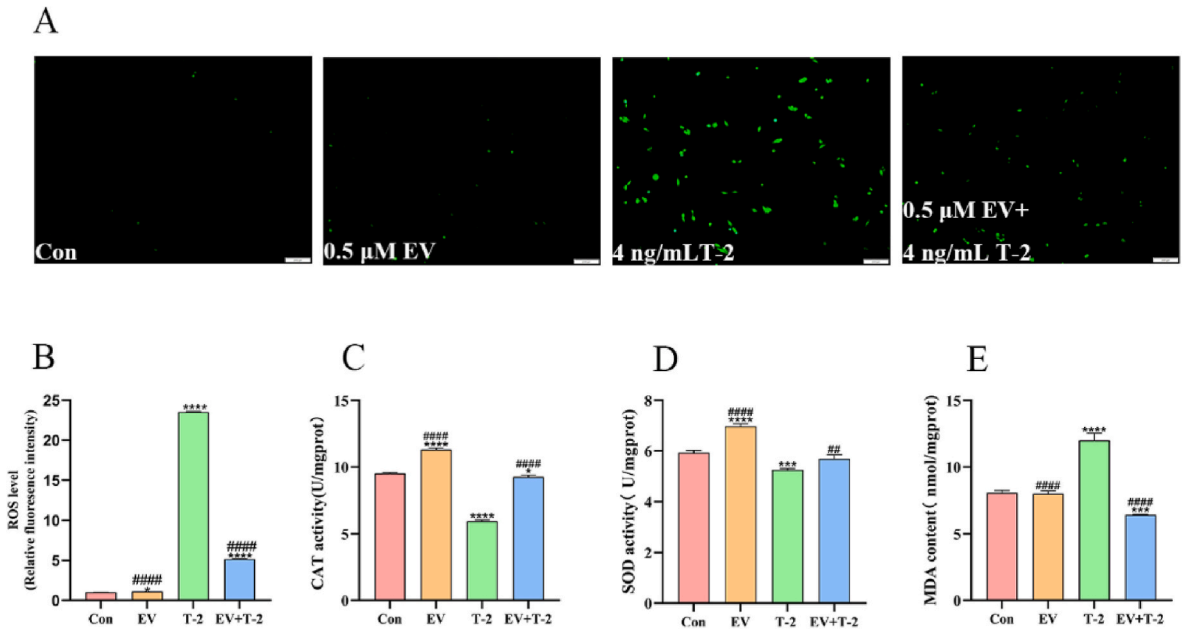

Fig. 2. Effect of EV on T-2-indued oxidative stress in IPEC-J2 cells. (A–B) The intracellular ROS levels. (C–E) The CAT and SOD activities, and the MDA connect. Data are presented as mean ± SD (n = 3). *p < 0.05, **p < 0.01, ***p < 0.001 and ****p < 0.0001 vs. control; #p < 0.05, ##P < 0.01, ###p < 0.001 and ####p < 0.0001 vs. T-2.

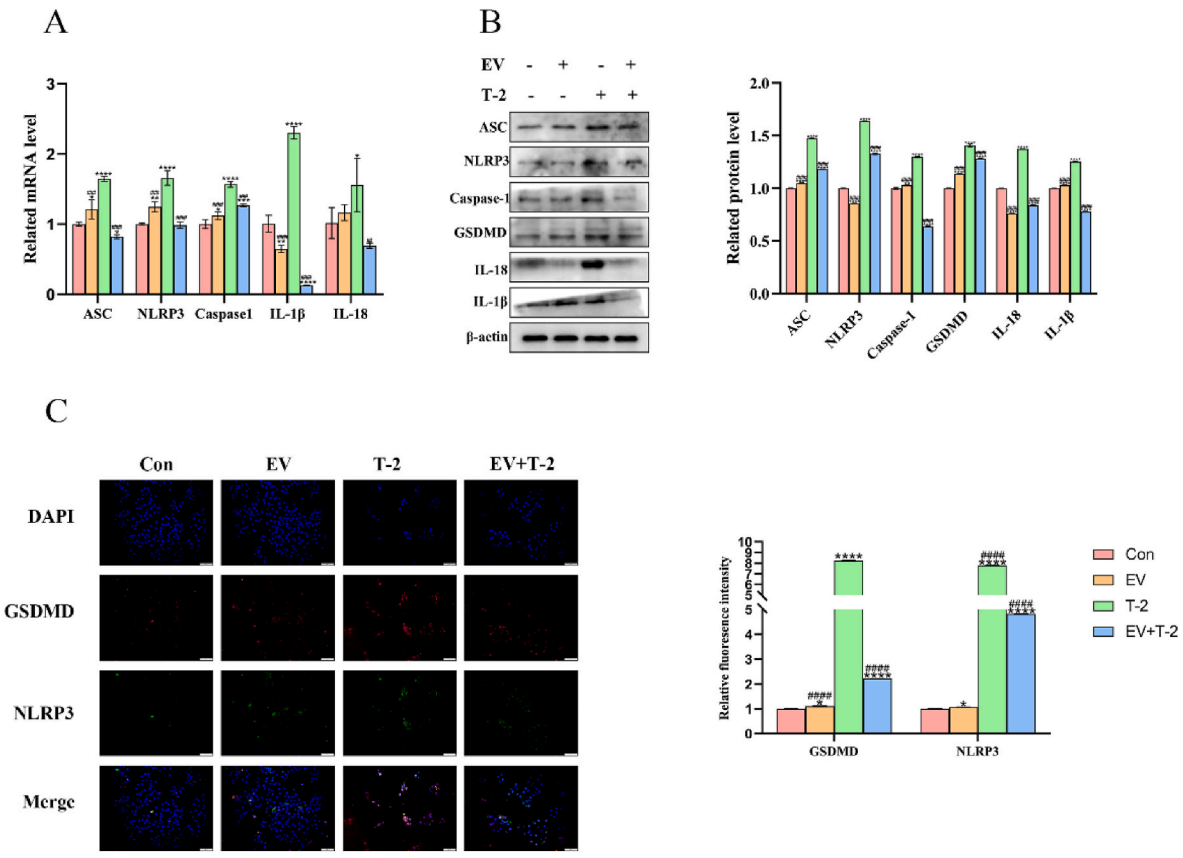

Fig. 3. Effect of EV on T-2-induced pyroptosis in IPEC-J2 cells. (A) The mRNA levels of ASC, NLRP3, caspase-1, IL-1β, and IL-18. (B) The protein expression of ASC, NLRP3, caspase-1, GSDMD, IL-1β, and IL-18. (C) Immunofluorescence images of GSDMD and NLRP3. Red and green fluorescence respectively indicate GSDMD and NLRP3 signals in IPEC-J2 cells. Data are presented as mean ± SD (n = 3). *p < 0.05, **p < 0.01, ***p < 0.001 and ****p < 0.0001 vs. control; #p < 0.05, ##p < 0.01, ###p < 0.001 and ####p < 0.0001 vs. T-2.

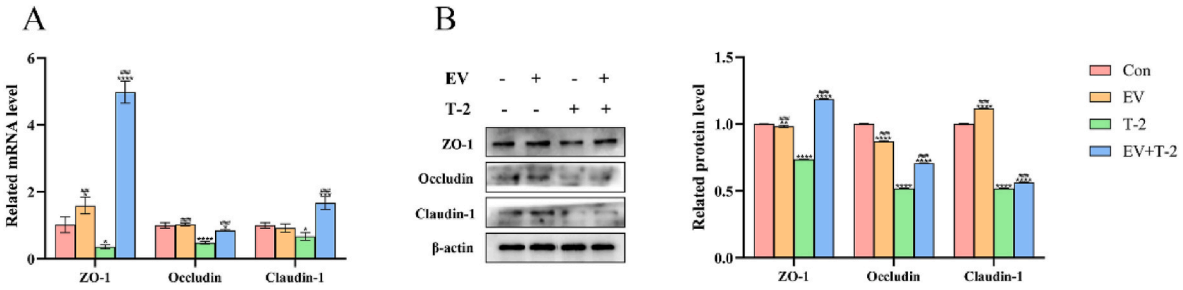

Fig. 4. Effect of EV on T-2-induced disorder of tight junction in IPEC-J2 cells. (A) The mRNA levels of ZO-1, occludin, and claudin-1. (B) The protein expresses of ZO-1, occludin, and claudin-1. Data are presented as mean ± SD (n = 3). *p < 0.05, **p < 0.01, ***p < 0.001 and ****p < 0.0001 vs. control; #p < 0.05, ##p < 0.01, ###p < 0.001 and ####p < 0.0001 vs. T-2.

3.5. EV treatment weakened the effect of T-2 exposure on Keap1-Nrf2/NF-κB signal pathway in IPEC-J2 cells

To ensure the impact of EV on the Keap1-Nrf2/NF-κB pathway induced by T-2, we assessed NF-κB and Nrf2 mRNA expression and measured the related protein expression. As exhibited in Fig. 5A–C, T-2 exposure led to a notable increase in the mRNA expression of NF-κB, up-regulated iκκα, p-NF-κB p65, nu-NF-κB p65, and cy-Nrf2 protein expression, decreased Nrf2 mRNA levels and down-regulated Keap1, cy-NF-κB p65, and nu-Nrf2 protein expression ($p < 0.0001$). Nevertheless, the EV could reverse T-2-induced results of the above mRNA and protein expression ($p < 0.01$). Thus, these results showed that EV could weaken the influence of T-2 on the Keap1-Nrf2/NF-κB signaling pathway though promoting Nrf2 into the nucleus.

3.6. Inhibition of Nrf2 by ML385 reversed the protective effect of EV against T-2-induced IPEC-J2 cell damage

To further investigate whether Nrf2 played a pivotal role in the process of EV alleviating IPEC-J2 cell injury triggered by T-2, EV, T-2 and ML385 (0.25 μM) co-treated IPEC-J2 cells for 24 h. ML385 was a specific Nrf2 inhibitor, which could reduce the Nrf2 transcriptional activity. As exhibited in Fig. 6A–C, the ML385 treatment induced a large increase in intracellular ROS accumulation. Additionally, the administration of ML385 caused a substantial reduction in Keap1 and nu-Nrf2 protein expression while dramatically up-regulated cy-Nrf2, p-NF-κB p65, and un-NF-κB p65 protein expression ($p < 0.0001$). Furthermore, ML385 reversed the effect of EV on the pyroptosis-associated proteins and intestinal tight junction protein expression ($p < 0.0001$, Fig. 6B).

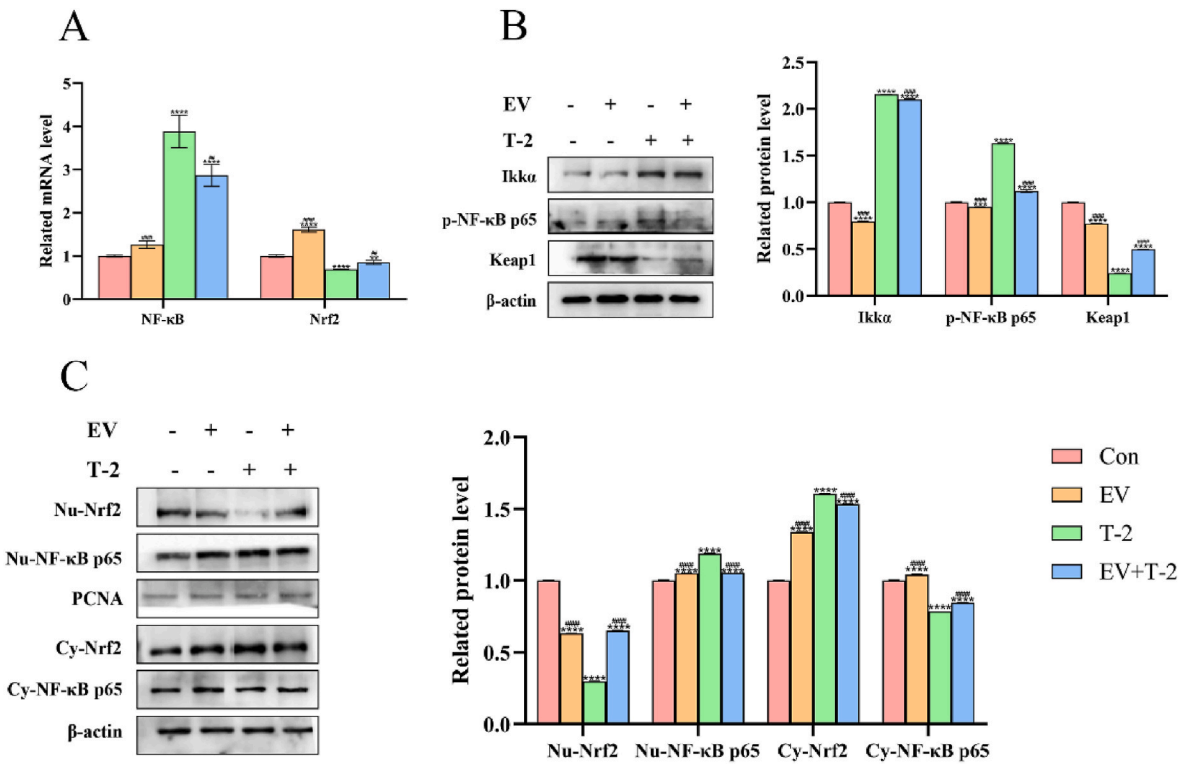

Fig. 5. Effect of EV on T-2-induced Keap1-Nrf2/NF-κB pathway in IPEC-J2 cells. (A) The mRNA levels of NF-κB and Nrf2. (B) The protein expression of ikkα, p-NF-κB p65 and Keap1. (C) The protein expression of nu-Nrf2, nu-NF-κB p65, cy-Nrf2 and nu-NF-κB p65. Data are presented as mean ± SD (n = 3). *p < 0.05, **p < 0.01, ***p < 0.001 and ****p < 0.0001 vs. control; $^{\#}$p < 0.05, $^{\#\#}$p < 0.01, $^{\#\#\#}$p < 0.001 and $^{\#\#\#\#}$p < 0.0001 vs. T-2.

These results suggested that EV could regulate the Keap1-Nrf2/NF-κB signaling pathway, reduce the production of ROS and ultimately alleviate the T-2-induced IPEC-J2 cells pyroptosis and intestinal barrier damage.

3.7. Enrichment clustering, PPI analysis and molecular docking analysis

According to the GO analyses of differentially expression genes, performed using Metascape, the genes were mainly enriched in NLRP3 inflammasome complex, cellular response to cytokine stimulus, regulation of proteolysis, non-canonical NF-κB signal transduction and others (Fig. 7A–C). Meanwhile, we constructed a functional PPI network, using the STRING database, composed of proteins related to intestinal tight junction dysfunction, Keap1-Nrf2 signaling pathway, NF-κB signaling pathway and pyroptosis (Fig. 7D). The network revealed the intrinsic links between the aforementioned proteins.

To further clarity the mechanism of EV on the Keap1-Nrf2/NF-κB signaling pathway, we successfully constructed the model of the EV-Keap1 complex using AutoDock Vina software. As presented in Fig. 7E, the hydrogen bond and hydrophobic force played a main role in the binding of EV interacting with Keap1. EV formed two hydrogen bonds with Val-418 and Val-561of Keap1, whose lengths were 2.75 Å and 2.60 Å, respectively. In addition, there was Pi-Alkyl hydrophobic force between EV and Ala-366, Val-369, and Ala-609 of Keap1. The binding energy of EV and Keap1 was −9.5 kcal/mol, which proved that EV on Keap1 had an excellent binding effect. Taken together, the potential mechanism behind the protective action of EV on T-2-triggered IPEC-J2 cell injury might be completed by binding to Keap1 to promote Nrf2 entry into the nucleus. Activated Nrf2, on the one hand, directly inhibits the entry of NF-κB into the nucleus and, on the other hand, indirectly down-regulates the expression of NF-κB by reducing intracellular ROS production.

4. Discussion

T-2 toxin is regarded as the most highly toxic of the trichothecenes (Eriksen and Pettersson, 2004). Due to its wide distribution, strong toxicity, strong carcinogenic, teratogenic, and mutagenic effects (Adhikari, Negi et al. 2017), T-2 has posed a significant risk to both human and animal well-being and has become a major food safety concern. Numerous studies have verified that swine has the highest level of sensitivity to T-2, which can affect the feed intake of pigs, destroy the integrity of the intestine, produce OS, mitochondrial damage, and inflammatory response (Goossens, Pasmans et al. 2012; Chen, Wang et al. 2023). EV is an indole alkaloid derived from the Chinese herb botanical species Evodia officinalis. According to reports, EV can effectively reduce colitis and colon cancer induced by azomethane/dextran sulfate sodium in mice by regulating intestinal inflammation (Wang, Zhou et al. 2021). Nevertheless, the protective action of EV-mitigated cell injury generated by T-2 is uncertain. Hence, IPEC-J2 cells as a model in the present study were used to explore the potential protective effect and mechanism of EV on IPEC-J2 cells damage induced y T-2, as well as the effect of EV on Keap1-Nrf2/NF-κB signaling pathway. The findings of our study demonstrated that exposure to T-2 decreased IPEC-J2 cell viability, enhanced LDH activity, significantly induced OS, blocked the Keap1-Nrf2/NF-κB signaling pathway, down-regulated tight junction protein expression, and triggered IPEC-J2 cell pyroptosis mediated by caspase-1. Meanwhile, EV activated the Keap1-Nrf2/NF-κB signaling pathway by binding to Keap1, decreased intracellular OS, up-regulated the expression of tight junction protein, and alleviated pyroptosis caused by T-2. However, ML385 reversed the therapeutic effect of EV. Overall, our results demonstrated the ability of EV to counter T-2-induced IPEC-J2 cell cytotoxicity.

OS refers to a severe imbalance between the reactive species (RS) produced and the antioxidant defenses (Halliwell, 2007, Gao, Yang et al. 2022a; Gao, Zhu et al. 2022b), which can be caused by excessive production of ROS during metabolism (Birben, Sahiner et al. 2012; Lu et al.,

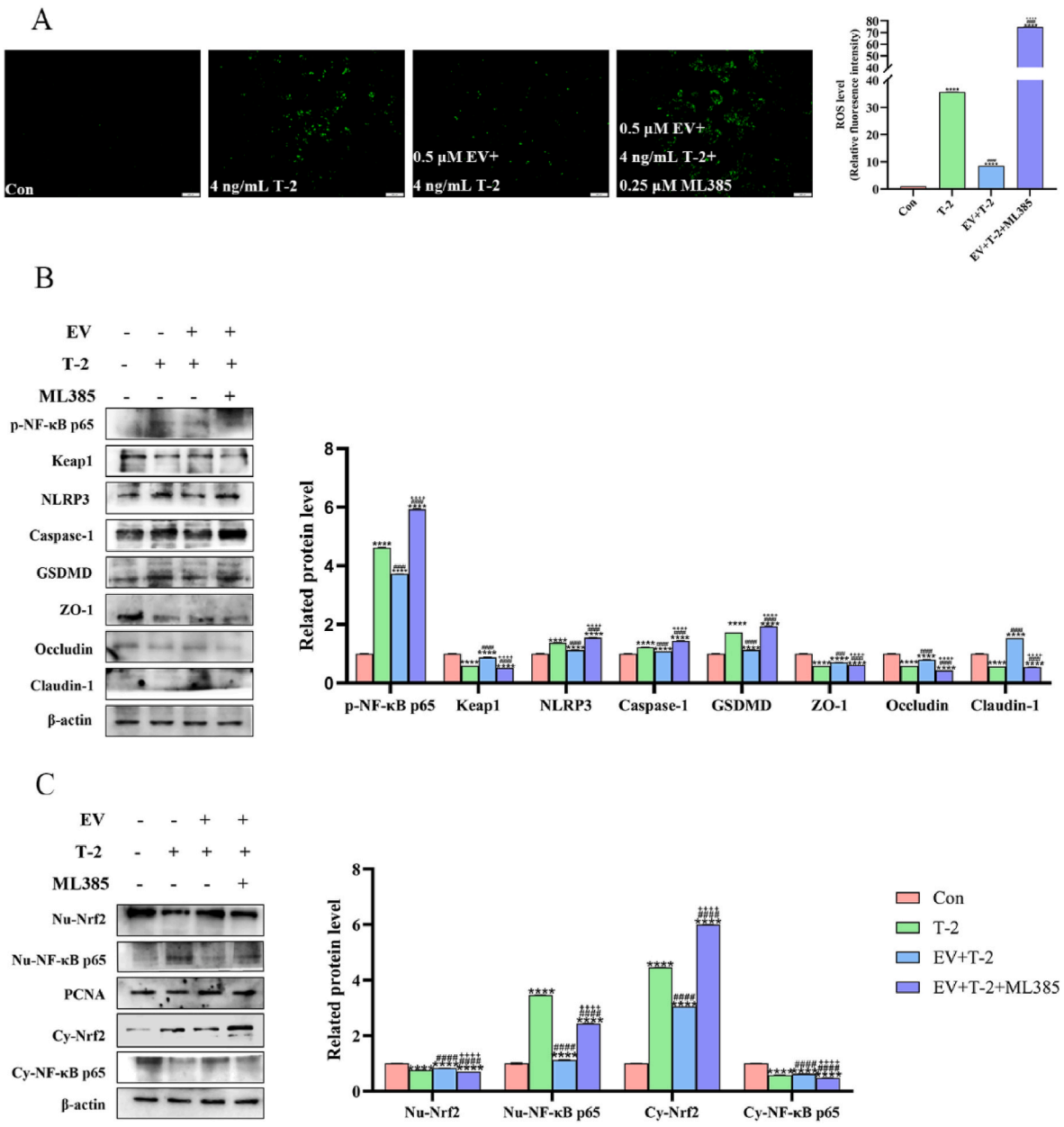

Fig. 6. Inhibition of Nrf2 by ML385 reversed the protective impact of EV on T-2-induced in IPEC-J2 cell injury. (A) The intracellular ROS levels. (B) The protein expression of p-NF-κB p65, Keap1, NLRP3, caspase-1, GSDMD, ZO-1, occludin, claudin-1. (C) The protein expression of nu-Nrf2, nu-NF-κB p65, cy-Nrf2 and nu-NF-κB p65. Data are presented as mean ± SD (n = 3). *p < 0.05, **p < 0.01, ***p < 0.001 and ****p < 0.0001 vs. control; $^{\#}$p < 0.05, $^{\#\#}$p < 0.01, $^{\#\#\#}$p < 0.001 and $^{\#\#\#\#}$p < 0.0001 vs. T-2; $^{+}$p < 0.05, $^{++}$p < 0.01, $^{+++}$ p < 0.001 and $^{++++}$P < 0.001 vs. EV and T-2 combination.

2022). Toxicants such as cadmium zearalenone and DEHP can exert various toxic effects by causing OS (Lopez, Arce et al. 2006; Hassen, Ayed-Boussema et al. 2007; Tsai, Wu et al. 2022). We observed that T-2 increased intracellular ROS levels, decreased SOD and CAT activity, and markedly increased MDA content, indicating that IPEC-J2 cells underwent intense OS. Simultaneously, numerous studies have claimed that OS can induce pyroptosis (Diao, Chen et al. 2019; Liu, Du et al. 2020a,b; Pei, Jiang et al. 2023). In the same way, the pyroptosis-associated gene expression enhanced after T-2 exposure. Additionally, In vitro and in vivo studies have demonstrated that EV can enhance antioxidant enzyme activities to inhibit OS and detoxify through the Nrf2 and MAPK signaling pathways (Xu et al., 2022; Lei, Zhang et al. 2023). We found that EV treatment inhibited intracellular ROS production and MDA accumulation, while SOD and CAT activities increased significantly. Those findings suggested that EV might alter the elevated ROS levels in IPEC-J2 cells caused by T-2 exposure by increasing SOD and CAT activities. At the same time, we found that EV inhibited the pyroptosis of IPEC-J2 cells by decreasing pyroptosis-associated protein/mRNA expression. Thus, these findings indicate that EV protects IPEC-J2 cells against T-2 by activating the antioxidant system.

Intestinal epithelial cells are the essential components of the body' s immune barrier, and tight junction protein serves a pivotal role in maintaining the integrity and function of the intestinal barrier. Research has demonstrated that T-2 possesses the capacity to damage intestinal barrier function (Liu, Yang et al. 2020; Luo, Huang et al. 2020). Consistent with our findings, ZO-1, occludin, and claudin-1 mRNA and protein expression dropped after exposure to T-2 for 24 h. In our experiment, EV was able to reduce the intracellular OS levels. We also found that EV could restore intestinal barrier function by up-regulating tight junction mRNA/protein expression. Thus, we further demonstrated

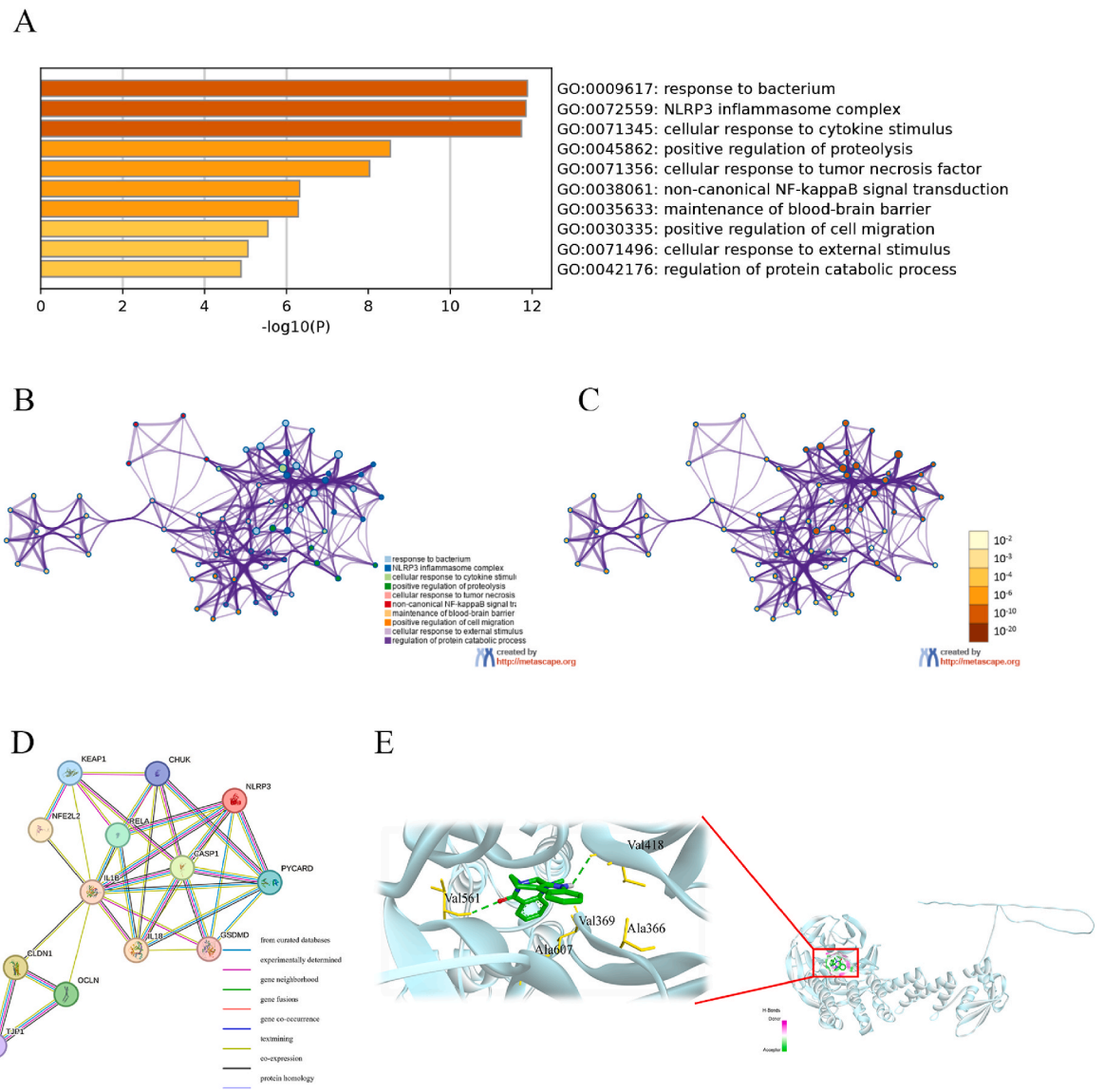

Fig. 7. Enrichment analysis, PPI network analysis and Molecular docking. (A–C) Bar graph of enriched terms across differentially expressed proteins, Using Metascape, colored by P value. Rich term networks colored by cluster or P value, using the same color for the same cluster. The darker the color, the more significant the P value. (D) The PPI network of differentially expressed proteins based on STRING database. (E) The three-dimensional binding model of the Keap1 protein and the EV ligand. EV shows the green stick structure, Keap1 shows a sky-blue folded structure, bond keys show the dotted lines, and the letter-number type annotations are the residue name of the protein.

that EV might enhance intestinal barrier function by clearing T-2-induced intracellular ROS.

Nrf2 and NF-κB, a transcription factor that mainly regulates oxidation-reduction, play an essential role in OS (Sies, Berndt et al. 2017; Hou, Wang et al. 2022). Meanwhile, Nrf2 and NF-κB can modulate each other, and some studies found that NF-κB showed more significant activity in Nrf2 gene knockout cells, and NF-κB also negatively regulated Nrf2 (Pan, Wang et al. 2012). Nrf2 and NF-κB are closely related to pyroptosis and OS. For example, lithium up-regulates NF-κB and NLRP3 inflammasome expression through OS, ultimately leading to pyroptosis in renal cells (Jing, Wang et al. 2022); diosmetin reduces periodontitis by suppressing OS and pyroptosis through Nrf2/NF-κB/NLRP3 axis (Cheng, Wang et al. 2022). Hence, in this study we tested whether the Keap1-Nrf2/NF-κB signaling pathway involved in the detoxification of EV on T-2. Surprisingly, we observed that after T-2 exposure, the expression of Keap1 protein was significantly decreased, Nrf2 protein expression notably reduced in the nucleus and increased in the cytoplasm, while the NF-κB protein expression in the nucleus and cytoplasm was opposite. Meanwhile, EV treatment reversed the results of the above mRNA and protein expression caused by T-2. This phenomenon might be related to the activation of Keap1-Nrf2/NF-κB signaling pathway by EV treatment, which activated Nrf2, inhibited the NF-κB shift into the nucleus, and then maintained intracellular redox homeostasis. To confirm the idea, we added ML385, a specific inhibitor of Nrf2, to IPEC-J2 cells while exposed to T-2 and EV. It was found that ML385 markedly increased intracellular ROS and intranuclear NF-κB p65 expression levels and decreased Keap1 and intranuclear Nrf2 expression. In addition, when ML385, EV and T-2 were treated together, ML385 reversed the protective impact of EV on T-2-induced IPEC-J2 cells pyroptosis and intestinal barrier. Therefore, the protective effect of EV is related to the activation of Keap1-Nrf2/NF-κB signaling pathway to reduce ROS accumulation. Our PPI network suggested that the Keap1-Nrf2 signaling pathway can inhibit pyroptosis by regulating NF-κB, and ultimately maintain gastrointestinal barrier function though reducing the production of inflammatory factors. In order to further clarify the molecular mechanism of Keap1-Nrf2 pathway regulated by EV, we used the

molecular docking method to successfully construct the EV-Keap1 complex model, whose binding energy is −9.5 kcal/mol, indicating that EV can bind Keap1 well. The findings of this study suggested that the Keap1-Nrf2/NF-κB signaling pathway is essential for EV to mitigate T-2-induced IPEC-J2 cell injury. And EV binds to Keap1 to activate Nrf2/NF-κB signaling pathway, promote Nrf2 entry into the nucleus, and inhibit NF-κB shift to the nucleus, reduce the generation of intercellular oxidative stress, thereby reducing the T-2-induced IPEC-J2 cells pyroptosis, and restoring intestinal tight junction dysfunction.

5. Conclusion

In conclusion, T-2 can inhibit Nrf2 entry into the nucleus, promote the NF-κB shift to the nucleus, induce OS, up-regulate pyroptosis-related gene expression, mediate pyroptosis of IPEC-J2 cells, and thus destroy intestinal barrier function. In addition, we demonstrate that EV has a significant protective action against T-2-induced IPEC-J2 cell injury. The mechanism action of EV might be to enhance the entry of Nrf2 into the nucleus through binding with Keap1. Activated Nrf2 has dual effects. It can directly inhibit pyroptosis by suppressing the expression of NF-κB. In addition, it can reduce intracellular ROS production to indirectly down-regulate NF-κB expression, thereby inhibiting pyroptosis. The implication of these results is that EV can alleviate the IPEC-J2 cells' pyroptosis caused by T-2, which is achieved by the activation of the Keap1-Nrf2/NF-κB signaling pathway. This study presents a novel approach for expanding the range of applications for EV and T-2 detoxification.

Funding

The authors declare that no funds, grants, or other support were received during the preparation of this manuscript.

Ethical approval

Not applicable.

Consent to participate

Informed consent was obtained from all individual participants included in the study.

Consent for publication

All authors declare consent of publication.

CRediT authorship contribution statement

Tingting Yu: Writing – original draft, Validation, Investigation. **Xinrui Deng:** Validation, Investigation. **Xuejiao Yang:** Visualization, Software, Data curation. **Yilin Yin:** Visualization, Software, Data curation. **Yong Liu:** Writing – review & editing, Conceptualization. **Shiwen Xu:** Writing – review & editing, Supervision, Conceptualization.

Declaration of competing interest

The authors declare that they have no known competing financial interests or personal relationships that could have appeared to influence the work reported in this paper.

Data availability

Data will be made available on request.

References

Adhikari, M., Negi, B., Kaushik, N., Adhikari, A., Al-Khedhairy, A.A., Kaushik, N.K., Choi, E.H., 2017. T-2 mycotoxin: toxicological effects and decontamination strategies. Oncotarget 8 (20), 20.
Ahmed, S.M.U., Luo, L., Namani, A., Wang, X.J., Tang, X., 2017. Nrf2 signaling pathway: pivotal roles in inflammation. Biochimica et Biophysica Acta -Molecular Basis of Disease 1863 (2), 13.
Barnabei, L., Laplantine, E., Mbongo, W., Rieux-Laucat, F., Weil, R., 2021. NF-κB: at the borders of autoimmunity and inflammation. Front. Immunol. 12, 27.
Birben, E., Sahiner, U.M., Sackesen, C., Erzurum, S., Kalayci, O., 2012. Oxidative stress and antioxidant defense. World Allergy Organization Journal 5, 11.
Chen, F.J., Wang, Y.S., Chen, Y.H., Fan, J.Y., Zhang, C., He, X.Y., Yang, X., 2023. JNK molecule is a toxic target for IPEC-J2 cell barrier damage induced by T-2 toxin. Ecotoxicol. Environ. Saf. 263, 11.
Cheng, M., Wang, P., Wu, D., 2022. Diosmetin alleviates periodontitis by inhibiting oxidative stress and pyroptosis through Nrf2/NF κB/NLRP3 axis. Trop. J. Pharmaceut. Res. 21 (12), 6.
Čonková, E., Laciakova, A., Kováč, G., Seidel, H., 2003. Fusarial toxins and their role in animal diseases. Vet. J. 165 (3), 214–220.
De Nicola, G.M., Karreth, F.A., Humpton, T.J., Gopinathan, A., Wei, C., Frese, K., Mangal, D., Yu, K.H., Yeo, C.J., Calhoun, E.S., Scrimieri, F., Winter, J.M., Hruban, R. H., Iacobuzio-Donahue, C., Kern, S.E., Blair, I.A., Tuveson, D.A., 2011. Oncogene-induced Nrf2 transcription promotes ROS detoxification and tumorigenesis. Nature 475 (7354), 4.
Diao, C.H., Chen, Z.Y., Qiu, T., Liu, H., Yang, Y.Y., Liu, X.H., Wu, J.F., Wang, L., 2019. Inhibition of PRMT5 attenuates oxidative stress-induced pyroptosis via activation of the Nrf2/HO-1 signal pathway in a mouse model of renal ischemia-reperfusion injury. Oxidative Medicine and Cellular Longevity 2019 18.
Dolcet, X., Llobet, D., Pallares, J., Matias-Guiu, X., 2005. NF-kB in development and progression of human cancer. Virchows Arch. 446 (5), 8.
Dong, Z., Yang, B., Jia, M., Yang, C., Wang, S., Mu, H., Wang, J.J. B.e. b. a.M.c. r., 2024. DDIT3/CHOP Promotes LPS/ATP-induced Pyroptosis in Osteoblasts via Mitophagy Inhibition, 119712.
Eriksen, G.S., Pettersson, H., 2004. Toxicological evaluation of trichothecenes in animal feed. Animal Feed Science and Technolog 114 (1–4), 35.
Gao, M., Yang, N., Lei, Y., Zhang, W., Liu, H., Lin, H.J.F., immunology, s., 2022a. Tannic acid antagonizes atrazine exposure-induced autophagy and DNA damage crosstalk in grass carp hepatocytes via NO/iNOS/NF-κB signaling pathway to maintain stable immune function, 131, 1075–1084.
Gao, M., Zhu, H., Guo, J., Lei, Y., Sun, W., Lin, H., 2022b. Tannic acid through ROS/TNF-α/TNFR 1 antagonizes atrazine induced apoptosis, programmed necrosis and immune dysfunction of grass carp hepatocytes. Fish Shellfish Immunol. 131, 312–322.
Goossens, J., Pasmans, F., Verbrugghe, E., Vandenbroucke, V., De Baere, S., Meyer, E., Haesebrouck, F., De Backer, P., Croubels, S., 2012. Porcine intestinal epithelial barrier disruption by the Fusarium mycotoxins deoxynivalenol and T-2 toxin promotes transepithelial passage of doxycycline and paromomycin. BMC Vet. Res. 8, 10.
Halliwell, B., 2007. Biochemistry of oxidative stress. Biochem. Soc. Trans. 35, 4.
Hassen, W., Ayed-Boussema, I., Oscoz, A.A., Lopez, A.D.C., Bacha, H., 2007. The role of oxidative stress in zearalenone-mediated toxicity in Hep G2 cells: oxidative DNA damage, gluthatione depletion and stress proteins induction. Toxicology 232 (3), 9.
Hou, L., Wang, D., Yin, K., Zhang, Y., Lu, H., Guo, T., Li, J., Zhao, H., Xing, M., 2022. Polystyrene microplastics induce apoptosis in chicken testis via crosstalk between NF-κB and Nrf2 pathways. Comparative Biochemistry and Physiology C-Toxicology & Pharmacology 262, 109444.
Hurtado-Navarro, L., Angosto-Bazarra, D., Pelegrin, P., Baroja-Mazo, A., Cuevas, S., 2022. NLRP3 inflammasome and pyroptosis in liver pathophysiology: the emerging relevance of Nrf2 inducers. Antioxidants 11 (5), 16.
Jiang, J., Hu, C., 2009. Evodiamine: a novel anti-cancer alkaloid from Evodia rutaecarpa. Molecules 14 (5), 8.
Jing, H., Wang, F., Gao, X., 2022. Lithium intoxication induced pyroptosis via ROS/NF-κB/NLRP3 inflammasome regulatory networks in kidney of mice. Environ. Toxicol. 37 (4), 11.
Kansanen, E., Kuosmanen, S.M., Leinonen, H., Levonen, A.L., 2013. The Keap1-Nrf2 pathway: mechanisms of activation and dysregulation in cancer. Redox Biol. 1 (1), 5.
Lei, Y.T., Zhang, W.Y., Gao, M.C., Lin, H.J., 2023. Mechanism of evodiamine blocking Nrf2/MAPK pathway to inhibit apoptosis of grass carp hepatocytes induced by DEHP. Comparative Biochemistry and Physiology C-Toxicology & Pharmacology 263, 9.
Li, J., Yin, K., Hou, L., Zhang, Y., Lu, H., Ma, C., Xing, M., 2023. Polystyrene microplastics mediate inflammatory responses in the chicken thymus by Nrf2/NF-κB pathway and trigger autophagy and apoptosis. Environ. Toxicol. Pharmacol. 100, 104136.
Li, S., Gu, X., Zhang, M., Jiang, Q., Xu, T., 2024. Di (2-ethylhexyl) phthalate and polystyrene microplastics co-exposure caused oxidative stress to activate NF-κB/NLRP3 pathway aggravated pyroptosis and inflammation in mouse kidney. Sci. Total Environ. 926, 171817.
Li, Y.S., Wang, Z.H., Beier, R.C., Shen, J.Z., De Smet, D., De Saeger, S., Zhang, S.X., 2011. T-2 toxin, a trichothecene mycotoxin: review of toxicity, metabolism, and analytical methods. J. Agric. Food Chem. 59 (8), 13.
Liu, S.S., Du, J., Li, D.F., Yang, P.P., Kou, Y.Y., Li, C.S., Zhou, Q., Lu, Y.P., Hasegawa, T., Li, M.Q., 2020a. Oxidative stress induced pyroptosis leads to osteogenic dysfunction of MG63 cells. J. Mol. Histol. 51 (3), 12.

Liu, Y.M., Yang, Y.X., Dong, R.Q., Zhang, Z.X., Jia, F.F., Yu, H.T., Wang, Y.Q., Zhang, Z. Q., 2020b. Protective effect of selenomethionine on intestinal injury induced by T-2 toxin. Res. Vet. Sci. 132, 9.
Lopez, E., Arce, C., Oset-Gasque, M.J., Canadas, S., Gonzalez, M.P., 2006. Cadmium induces reactive oxygen species generation and lipid peroxidation in cortical neurons in culture. Free Radic. Biol. Med. 40 (6), 12.
Lu, H., Guo, T., Zhang, Y., Liu, D., Hou, L., Ma, C., Xing, M., 2024. Endoplasmic reticulum stress-induced NLRP3 inflammasome activation as a novel mechanism of polystyrene microplastics (PS-MPs)-induced pulmonary inflammation in chickens. J. Zhejiang Univ. - Sci. B 25 (3), 233–243.
Lu, H., Su, H., Liu, Y., Yin, K., Wang, D., Li, B., Wang, Y., Xing, M., 2022. NLRP3 inflammasome is involved in the mechanism of the mitigative effect of lycopene on sulfamethoxazole-induced inflammatory damage in grass carp kidneys. Fish Shellfish Immunol. 123, 348–357.
Luo, C., Huang, C., Zhu, L., Kong, L., Yuan, Z., Wen, L., Li, R., Wu, J., Yi, J., 2020. Betulinic acid ameliorates the T-2 toxin-triggered intestinal impairment in mice by inhibiting inflammation and mucosal barrier dysfunction through the NF-κB signaling pathway. Toxins 12 (12), 15.
Mahato, D., Pandhi, S., Kamle, M., Gupta, A., Sharma, B., Panda, B., Srivastava, S., Kumar, M., Selvakumar, R., Pandey, A., Suthar, P., Arora, S., Kumar, A., Gamlath, S., Bharti, A., Kumar, P., 2022. Trichothecenes in food and feed: occurrence, impact on human health and their detection and management strategies. Toxicon : official journal of the International Society on Toxinology 208, 15.
Mateo, J., Mateo, R., Jiménez, M., 2002. Accumulation of type A trichothecenes in maize, wheat and rice by Fusarium sporotrichioides isolates under diverse culture conditions. Int. J. Food Microbiol. 72 (1–2), 9.
Nathanail, A.V., Varga, E., Meng-Reiterer, J., Bueschl, C., Michlmayr, H., Malachova, A., Fruhmann, P., Jestoi, M., Peltonen, K., Adam, G., 2015. Metabolism of the Fusarium mycotoxins T-2 toxin and HT-2 toxin in wheat. J. Agric. Food Chem. 63 (35), 7862–7872.
Ogasawara, M., Matsunaga, T., Takahashi, S., Saiki, I., Suzuki, H., 2002. Anti-invasive and metastatic activities of evodiamine. Biological pharmaceutical bulletin 25 (11), 1491–1493.
Onodera, Y., Motohashi, H., Takagi, K., Miki, Y., Shibahara, Y., Watanabe, M., Ishida, T., Hirakawa, H., Sasano, H., Yamamoto, M., Suzuki, T., 2014. NRF2 immunolocalization in human breast cancer patients as a prognostic factor. Endocr. Relat. Cancer 21 (2), 12.
Pan, H., Wang, H., Wang, X., Zhu, L., Mao, L., 2012. The absence of nrf2 enhances nf-b-dependent inflammation following scratch injury in mouse primary cultured astrocytes. Mediat. Inflamm. 2012, 9.
Pei, X.Y., Jiang, H.Y., Li, C., Li, D.W., Tang, S.S., 2023. Oxidative stress-related canonical pyroptosis pathway, as a target of liver toxicity triggered by zinc oxide nanoparticles. J. Hazard Mater. 442, 18.
Rizzo, A., Atroshi, F., Ahotupa, M., Sankari, S., Elovaara, E., 1994. Protective effect of antioxidants against free radical-mediated lipid peroxidation induced by DON or T-2 toxin. J. Vet. Med. Ser. A 41 (1-10), 10.
Rousta, A., Mirahmadi, S., Shahmohammadi, A., Mehrabi, Z., Fallah, S., Baluchnejadmojarad, T., Roghani, M., 2022. Therapeutic potential of isorhamnetin following acetaminophen-induced hepatotoxicity through targeting NLRP3/NF-κB/Nrf2. Drug Research 72 (5), 10.
Shi, H.T., Li, S.L., Bai, Y.Y., Prates, L.L., Lei, Y.G., Yu, P.Q., 2018. Mycotoxin contamination of food and feed in China: occurrence, detection techniques, toxicological effects and advances in mitigation technologies. Food Control 91, 14.
Sies, H., Berndt, C., Jones, D.P., 2017. Oxidative stress. Annu. Rev. Biochem. 86, 715–748. R. D. Kornberg. Palo Alto, Annual Reviews.
Sivandzade, F., Prasad, S., Bhalerao, A., Cucullo, L., 2019. NRF2 and NF-κB interplay in cerebrovascular and neurodegenerative disorders: molecular mechanisms and possible therapeutic approaches. Redox Biol. 21, 16.
Song, W., Wang, Y., Huang, T., Liu, Y., Chen, F., Chen, Y., Jiang, Y., Zhang, C., Yang, X., 2023. T-2 toxin metabolism and its hepatotoxicity: new insights on the molecular mechanism and detoxification. Environmental Pollution 330, 121784.
Streit, E., Schatzmayr, G., Tassis, P., Tzika, E., Marin, D., Taranu, I., Tabuc, C., Nicolau, A., Aprodu, I., Puel, O., Oswald, I.P., 2012. Current situation of mycotoxin contamination and Co-occurrence in animal feed-focus on europe. Toxins 4 (10), 22.
Tsai, H., Wu, C., Hsiung, C., Lee, C., Wang, S., Chen, M., Chen, C., Huang, P., Wang, Y., Chen, Y., Chen, B., Chuang, Y., Hsieh, H., Wu, M., 2022. Longitudinal changes in oxidative stress and early renal injury in children exposed to DEHP and melamine in the 2011 Taiwan food scandal. Environ. Int. 158, 12.
Ueno, Y., 1984. Toxicological features of T-2 toxin and related trichothecenes. Toxicol. Sci. 4 (2Part2), 9.
Wang, M.X., Zhou, B.Q., Cong, W.H., Zhang, M., Li, Z.W., Li, Y., Liang, S.Y., Chen, K.J., Yang, D.P., Wu, Z.Z., 2021. Amelioration of AOM/DSS-Induced murine colitis-associated cancer by evodiamine intervention is primarily associated with gut microbiota-metabolism-inflammatory signaling Axis. Front. Pharmacol. 12, 18.
Wang, Y., Liu, S.L., Zheng, H., He, C.H., Zhang, H.B., 2013. T-2 toxin, zearalenone and fumonisin B-1 in feedstuffs from China. Food Addit. Contam. Part B-Surveillance 6 (2), 7.
Wardyn, J., Ponsford, A., Sanderson, C., 2015. Dissecting molecular cross-talk between Nrf2 and NF-κB response pathways. Biochem. Soc. Trans. 43 (4), 6.
Xu, M., Wang, W.H., Lu, W., Ling, X.Y., Rui, Q., Ni, H.B., 2022. Evodiamine prevents traumatic brain injury through inhibiting oxidative stress via PGK1/NRF2 pathway. Biomed. Pharmacother. 153, 10.
Yang, X., Liu, P.L., Cui, Y.L., Xiao, B.N., Liu, M.L., Song, M., Huang, W.Y., Li, Y.F., 2020. Review of the reproductive toxicity of T-2 toxin. J. Agric. Food Chem. 68 (3), 8.
Yang, Y., Ran, X., Wang, H., Chen, Y., Hou, S., Yang, Z., Fu, S., Liu, J., Hu, G., Guo, W., 2022. Evodiamine relieve LPS-induced mastitis by inhibiting AKT/NF-κB p65 and MAPK signaling pathways. Inflammation 45 (1), 14.
Yao, Y.J., Chen, T., Wu, H., Yang, N.X., Xu, S.W., 2023. Melatonin attenuates bisphenol A-induced colon injury by dual targeting mitochondrial dynamics and Nrf2 antioxidant system via activation of SIRT1/PGC-1 alpha signaling pathway. Free Radic. Biol. Med. 195, 10.
Yu, H., Jin, H., Gong, W., Wang, Z., Liang, H., 2013. Pharmacological actions of multi-target-directed evodiamine. Molecules 18 (2), 18.
Yu, P., Zhang, X., Liu, N., Tang, L., Peng, C., Chen, X., 2021. Pyroptosis: mechanisms and diseases. Signal Transduct. Targeted Ther. 6 (1), 21.
Zhang, S., Song, W., Hua, Z., Du, J., Lucena, R.B., Wang, X., Zhang, C., Yang, X., 2024a. Overview of T-2 toxin enterotoxicity: from toxic mechanisms and detoxification to future perspectives. J. Agric. Food Chem. 72 (7), 3314–3324.
Zhang, Y., Zhang, E., Hou, L., Lu, H., Guo, T., Wang, R., Wang, Y., Xing, M., 2024b. Assessing and mitigating foodborne acetochlor exposure induced ileum toxicity in broiler chicks: the role of omega-3 polyunsaturated fatty acids supplementation and molecular pathways analysis. Pestic. Biochem. Physiol. 199, 105761.